

Simulation of Cosmic Radiation Transport Inside Aircraft for Safety Applications

ADRIANE CRISTINA MENDES PRADO 

MAURICIO TIZZIANI PAZIANOTTO

Technological Institute of Aeronautics, São José dos Campos, Brazil

JOSE MANUEL QUESADA MOLINA 

MIGUEL ANTONIO CORTES-GIRALDO 

Universidad de Sevilla, Seville, Spain

GUILLAUME HUBERT 

French Aerospace Lab (ONERA), Toulouse, France

MARLON ANTONIO PEREIRA

CLAUDIO ANTONIO FEDERICO 

Institute for Advanced Studies, São José dos Campos, Brazil

During the flight, an aircraft is submitted to a radiation environment composed of cosmic-ray-induced particles (CRIP) of which neutrons are responsible for approximately 40% of the crew effective

Manuscript received September 25, 2018; revised August 27, 2019 and November 26, 2019; released for publication January 28, 2020. Date of publication April 21, 2020; date of current version October 9, 2020.

DOI. No. 10.1109/TAES.2020.2985304

Refereeing of this contribution was handled by R. Sabatini.

This work was supported in part by the Coordination for the Improvement of Higher Education Personnel (CAPES), in part by the National Council on Research and Development (CNPq) under Projects 402209/2013-3 and 481432/2013-2, in part by FINEP under CITAR Project, and in part by the São Paulo Research Foundation (FAPESP) under Grant 2017/01886-3. The work of Miguel Antonio Cortés-Giraldo and José Manuel Quesada Molina was funded in part by the Spanish Ministry of Science, Innovation, and Universities under Research Projects FPA2016-77689-C2-1-R and RTI2018-098117-B-C21.

Authors' addresses: Adriane Cristina Mendes Prado is with the Technological Institute of Aeronautics, São José dos Campos 12228-900, Brazil, and also with the Institute for Advanced Studies, São José dos Campos 12228-001, Brazil, E-mail: (adriane@ieav.cta.br); Mauricio Tizziani Pazianotto is with the Technological Institute of Aeronautics, São José dos Campos 12228-900, Brazil, E-mail: (mtp@ita.br). Jose Manuel Quesada Molina and Miguel Antonio Cortes-Giraldo are with the Universidad de Sevilla, 41004 Seville, Spain, E-mail: (quesada@us.es; miancortes@us.es); Guillaume Hubert is with the French Aerospace Lab (ONERA), 31000 Toulouse, France E-mail: (guillaume.hubert@onera.fr); Marlon Antonio Pereira and Claudio Antonio Federico are with the Institute for Advanced Studies, São José dos Campos 12228-001, Brazil, E-mail: (marlon@ieav.cta.br; claudiofederico@ieav.cta.br). (*Corresponding author: Adriane Cristina Mendes Prado.*)

0018-9251 © 2020 CCBY

dose and are the main cause of single event effects (SEE) in avionics systems at flight altitudes. A model of Learjet aircraft was developed on Monte Carlo simulation using the MCNPX code in order to detail the CRIP field inside the aircraft. The radiation source modeling was previously developed by a computational platform that simulates the energy and angular distributions of the CRIP along the atmosphere. In this article, we determined the variation of the neutron radiation field in several positions inside the aircraft at 11- and 18-km altitudes and for both equatorial and polar regions. The results suggest that the maximum variation of neutron fluence rate between different positions inside the aircraft shows a tendency of higher differences for a lower energy threshold (thermal and $E > 1$ MeV) in comparison with those differences for a higher energy threshold ($E > 10$ MeV). Moreover, the angular distribution results show relevant differences between positions inside aircraft, mainly for thermal neutrons close to the fuel. The general tendency is to enhance these discrepancies for devices with new technologies, due to their lower energy threshold for SEE occurrences.

I. INTRODUCTION

The radiation environment at flight altitude is composed of several types of particles, i.e., neutrons, protons, photons, electrons, muons and pions, which are produced by interactions of primary cosmic radiation of solar and galactic origin with the constituents of the earth's atmosphere [1]. Among these various particles, the neutron is of fundamental importance in the aviation field, since it is the particle responsible for over 90% of the effects observed in embedded electronic systems and it is also responsible for most of the effective dose on aircraft crews. The radiation effect on electronic devices, called single event effect (SEE), is the main effect of neutrons in embedded electronics and it consists of the impact of a single particle, i.e., neutrons, protons, which deposit enough charge within a sensitive portion of a device to result in its malfunction [2].

During the last decade, the effects of ionizing radiation in avionics systems onboard aircraft became more important due to the advent of new technologies, the increase of air traffic, and the increase of flight altitudes. The increasing use of devices with even smaller feature size in avionics systems has led to an increased susceptibility of SEE [3]. Some studies suggest evaluating SEE failures in avionics, which should include, in addition to the susceptibility testing method with radiation sources, the investigation of the energy deposition in integrated circuits using Monte Carlo simulation, in order to evaluate the effects of radiation into its basic components [4] and the evaluation of the susceptibility to fast and thermal neutrons separately, since the latter can cause SEEs due to the interaction with boron, which is present in microelectronics [5].

Although the miniaturization of devices represents some technological progress, the radiation energy deposition thresholds are being reduced, leading to radiation with lower energy which can also cause SEEs.

In order to evaluate the SEE susceptibility of the cosmic-ray-induced neutron particle and the risk for air safety, it is important to quantify the radiation field inside aircraft, identifying its fluence spectra and angular distribution realistically. For this purpose, it is necessary to develop a computer model of aircraft and perform simulations of the

radiation transport through the aircraft submitted to the radiation environment at flight altitudes using Monte Carlo simulation.

Ferrari *et al.* [6], [7] developed a model of Airbus-340 and demonstrated that the shielding and thermalizing effects of aircraft structures and materials significantly influence the radiation levels on board, i.e., the dose can be different inside the aircraft depending on its location and the quantity of surrounding material. The results showed that the isotropic source is not a good approach and revealed that the effective dose due to upward-directed particles was reduced inside aircraft whereas the contribution of the downward-directed particle was slightly increased. Monte Carlo simulations made by Battistoni *et al.* [8] evaluated the radiation field behavior in a free atmosphere discussing the angular distribution and concluded that considering an isotropic radiation field, it could be a very poor approximation, as usual. Subsequently, Battistoni *et al.* [9] also found that the angular distribution depends on the particle energy and this fact has to be considered for the crew's dosimetry. Kubančák *et al.* [10] measured the ambient dose equivalent [$H^*(10)$] on board of three large aircraft and showed that $H^*(10)$ inside the cabin is lower than the dose measured in the front and in the back of the passenger's cabin. They also demonstrated that the fuel influences the $H^*(10)$, which is higher when the aircraft has a higher volumetric fuel capacity.

Experimental measurements of the neutron radiation field aboard aircraft were made by some authors on commercial aircraft, including Hubert *et al.* [11], Nakamura *et al.* [12], and Hewit [13] *et al.* However, only a few authors have experimentally evaluated variations in field behavior at various positions within the aircraft, due to the experimental difficulties involved. Significant computer simulation works on this topic were done by Dyer and Lei [3] and Ferrari *et al.* [6], [7].

This article aims to evaluate the cosmic-ray-induced neutron field inside a small aircraft with unprecedented detail of its energy and angular distribution using Monte Carlo simulations. This article evaluates the influence of structures and aircraft materials on the radiation field, studying the factors that provide greater internal radiation levels and consequently, greater susceptibility to failure of avionics devices, to use this data to predict radiation effects in avionics systems.

II. MATERIALS AND METHODS

This section describes the main aspects of the methodology developed for the evaluation of neutron fluence inside the aircraft, including the computational modeling of aircraft geometry and the radiation source at the atmosphere using the Monte Carlo code.

A. Model of the Aircraft

In order to investigate the influence of aircraft materials and structures on the ionizing radiation field from cosmic-

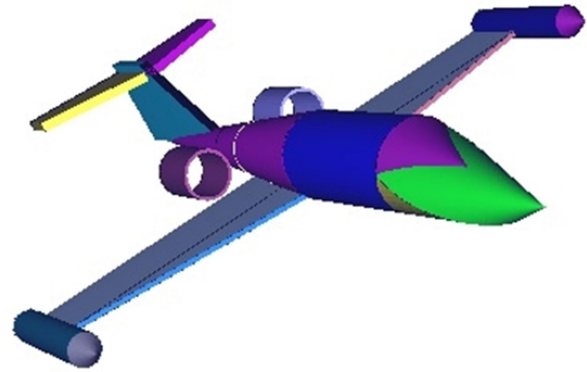


Fig. 1. Three-dimensional view of Learjet aircraft.

ray-induced particles inside an aircraft, a computational model of a Learjet-type aircraft was built based on Monte Carlo simulation using the MCNPX code [14].

The model reproduces a Learjet-35A with the real size and total mass of the real aircraft. According to Dalazen [15], the empty weight of the aircraft is 4152 kg and the maximum takeoff weight is 8165 kg. The simulated aircraft weighs 8159 kg.

The aircraft model was made in a simple way and consists of 58 cells and 12 different materials to describe its structure, material, and occupants. The geometry of the aircraft is detailed in a previous work [16] which demonstrates the validity of the simulations by comparing the ambient dose equivalent rate given by the aircraft Monte Carlo simulation results with experimental data taken in flight. From the results of the abovementioned work, we found that the experimental and simulated results are in good agreement within 3%, evidencing that, although the aircraft model was built simply, the set represented by the aircraft model and the methodology of the atmosphere radiation source is a good way to represent reality.

In the MCNPX input code, the materials were constructed from the isotopes of their constituent elements according to their atomic weight and isotopic composition as provided in NIST [17], using same proportions of material composition and density according to Ferrari *et al.* [7] and the nuclear data were taken from the Evaluated Nuclear Data Library (ENDF) [18].

Fig. 1 shows the 3-D view of the simulated Learjet aircraft model.

B. Flight Environment

Besides the construction of the aircraft geometry for the MCNPX code, it is also necessary to describe the radiation source, which represents the cosmic rays in the atmosphere. This simulation was made with a neutron source distributed uniformly over two flat surfaces delimited by a cylinder wall with reflective properties, which simulates one 3-D infinite atmospheric radiation environment using a finite geometry model, with the aircraft placed inside this volume. More details about the flight radiation environment and this methodology can be found in previous work [16].

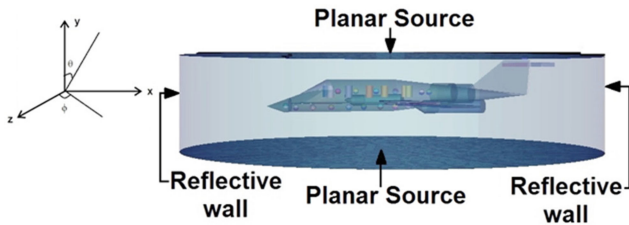


Fig. 2. Three-dimensional view of the complete geometry modeling of simulation.

The primary spectra and angular distributions at flight altitudes were obtained by the Geant4-based gPartAt platform [19], [20] using QGSP_BERT-HP physics list of Geant4.

This work evaluates two flight situations where a small aircraft is subjected to high and low doses of radiation, and thus, it is possible to relate it to the effect of the aircraft structure, fuel and passengers in the scattering of neutron radiation in different internal positions.

The first flight situation maximizes the neutron fluence in the atmosphere, i.e., it represents flights in the polar region (cutoff rigidity of 0 GV), at the solar minimum period (solar deceleration potential of 465 MV), both at 11- and 18-km of altitude. The second situation represents flights in the equatorial region (cutoff rigidity of 17 GV), in the solar maximum period (solar deceleration potential of 1700 MV), and in the same two preceding altitudes of flight; this situation minimizes the neutron fluence in the atmosphere. The 18-km altitude is well above the usual flight level for conventional aircraft, but it can be of interest to evaluate the operational ceiling for high-performance military aircraft and, also, may be an interesting preview for future hypersonic aircraft [21].

The radiation environment in these flight situations (primary particles come from the upper and lower surfaces of the containing volume) was obtained with the gPartAt application in which input data were specified for the same region and solar period.

The fluence rate ($\dot{\theta}$), quantity studied in this work, is given by (1), where θ is the neutron fluence per neutron-source per area (n/n-s.cm²), A_s is the source area (cm²) and F_{NF} is the normalizing factor that represents the integral planar fluence rate of neutron (n-s/cm².s)

$$\dot{\theta} = \theta \times 2 \times A_s \times F_{NF}. \quad (1)$$

The F_{NF} factor is calculated by gPartAt data and it is responsible for transforming the fluence, which is given by particle-source to fluence rate. Each source built on MCNPX has a different F_{NF} factor and depends on the number of neutrons obtained by gPartAt, which was originated from the primary protons and alphas from cosmic radiation incidents at the top of the atmosphere. The explanations of this equation and the F_{NF} factor are given in previous work [16].

Fig. 2 shows the complete geometry model used in Monte Carlo simulations, indicating the two planar sources

TABLE I
Input Data for gPartAt Platform

Situation	Parameters	Altitude
Minimizes the neutron fluence	Maximum solar period	11 km
	(1700 MV – 07/16/91); Equatorial region (17 GV -10 N,85 E)	18 km
Maximizes the neutron fluence	Minimum solar period	11 km
	(465 MV – 11/22/86); Polar region (0 GV – 90 N,0 E)	18 km

and the reflective cylindrical wall in which the aircraft is located in the center. This figure also shows the configuration within the aircraft, detailing the positions of the detectors and the cylinders, which represent the people onboard.

III. RESULTS AND DISCUSSION

A. Source Fluence

Equation (2) shows the source total fluence rate (θ_{TF}) calculated from gPartAt data

$$\theta_{TF} = \sum_{i=0}^{180^\circ} \left(\sum_{j=0}^{E_{\max}} \frac{\left[\left(\frac{p}{2} \times \varphi_{p,i,j} \right) + \left(\frac{a}{2} \times \varphi_{a,i,j} \right) \right]}{|\cos(\alpha_{\text{average}})|} \right) \quad (2)$$

where p and a are the integral fluence rate of the protons and alphas sources, obtained from gPartAt, respectively. φ_p and φ_a are the number of neutrons on a plane surface originated by the primary protons and alphas, respectively, given in neutron-source per proton-source (n-s/p-s) and neutron-source per alpha-source (n-s/a-s). α_{average} is the average angle of the angular range of the particles embedded in the source, j is the index of the binning in energy which ranges from 0 to E_{\max} , and i is the index of the binning in angle, which ranges from 0° to 180°, in intervals of 5°.

This equation converts the gPartAt results, given in the planar fluence [20], [22] into total fluence. The gPartAt platform generates the angular distribution of the cosmic-ray-induced particles at any altitude in the atmosphere and this information was considered to perform the simulations in the aircraft.

The input parameters that originated on gPartAt and used on MCNPX code are shown in Table I.

The altitude of 11-km was chosen because it is a typical flight altitude whereas the 18-km altitude is near the maximum of Pfozter. Table II shows the results of the total fluence obtained by gPartAt from (2), for each flight situation.

B. Fluence Rate Results as a Function of Position Inside Aircraft

The neutron fluence rate was calculated in different positions inside the Learjet aircraft, as shown in Fig. 3,

TABLE II
Neutron Total Fluence Rate of gPartAt Platform

Neutron Source and Flight Altitude		Total Fluence Rate (n/cm ² .s)
		gPartAt
0 GV 465 MV	11 km	6.61
	18 km	12.00
17 GV 1700 MV	11 km	0.76
	18 km	0.84

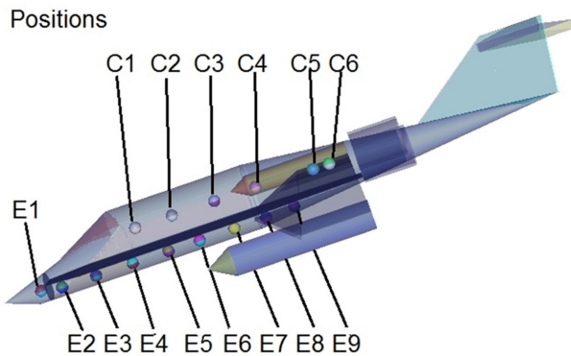


Fig. 3. Representation of the positions of the detectors inside the aircraft.

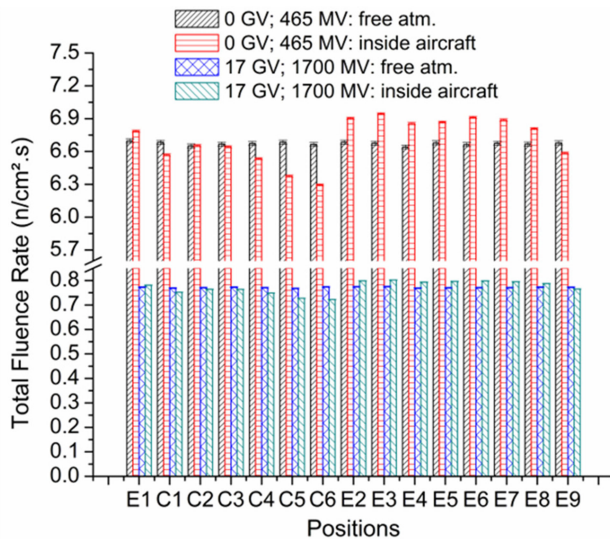


Fig. 4. Total fluence rate for 11-km of altitude.

distributed in Cabine positions (C) and Electronic bays positions (E).

1) *Fluence Rate Results as a Function of Position Inside Aircraft:* The total fluence rate is the integration of the fluence rate across the energy range and in all angular intervals, and it is shown in Fig. 4 at 11-km altitude and in Fig. 5 at 18-km altitude.

These figures compare the neutron fluence rate in the free atmosphere (atm.) with that one obtained at the positions inside the aircraft, as shown in Fig. 3 on each different flight conditions (11- and 18-km, respectively). The highest

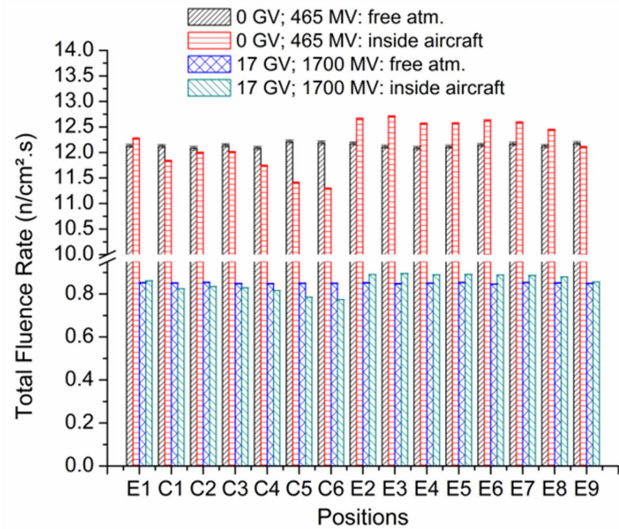


Fig. 5. Total fluence rate for 18-km of altitude.

total neutron fluence rate was at polar flights during solar minimum, for both altitudes evaluated.

The total fluence rate is higher inside the aircraft than in the free atmosphere for some evaluated positions. Some of the avionic devices are located in the E1 position inside the Learjet aircraft and in this position it is possible to observe the same behavior.

For the evaluation of the neutron SEE in electronics, it is important to evaluate the differential neutron fluence rate in energy. The SEE error rate is evaluated separately for thermal and high energy neutrons. Thermal neutrons, for example, should be carefully considered for radiation effects in avionics and high energy neutrons are also analyzed differently according to the geometric feature size of devices. Neutrons with energy greater than 10 MeV will be the dominant cause of SEE in devices which feature size is above 150 nm, while for devices with feature sizes at and below 150 nm, it is necessary to consider neutrons with energy greater than 1 MeV [2].

Figs. 6 and 7 show the thermal neutron fluence rate for different flight conditions and two altitudes, 11- and 18-km, respectively. The thermal neutrons fluence rate inside the aircraft structure presents is higher than at free atmosphere for almost all positions and both altitudes, with a maximum of about 2.9 times the fluence on the free atmosphere occurring at position C6, close to the fuel at 18-km altitude. The increase of thermal neutron fluence occurs for positions C1–C6, in which C1–C4 are near the people while C5 and C6 are near the fuel and at bottom of the aircraft, and in the position E9, due to the interaction of the neutrons with the aircraft fuel.

Figs. 8 and 9 show the neutron fluence rate with energy superior to 1 MeV, at 11- and 18-km altitude, respectively.

The neutron fluence rate for neutron energies above 1 MeV depends on their position and it is higher inside the aircraft than at free atmosphere for many positions evaluated. This behavior is found in electronic bays positions

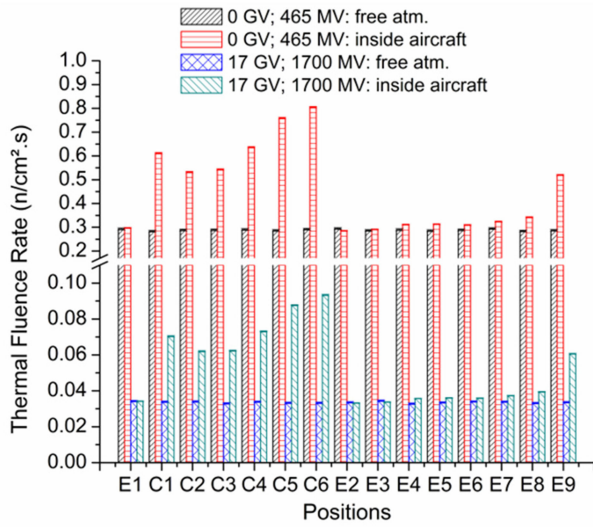


Fig. 6. Fluence rate of thermal neutron for 11-km of altitude.

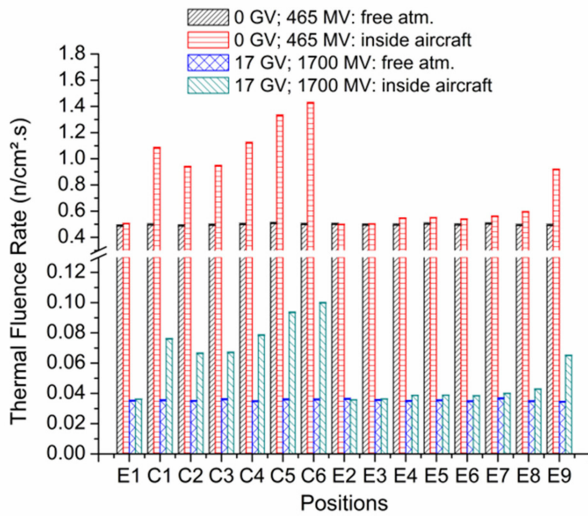


Fig. 7. Fluence rate of thermal neutron for 18-km of altitude.

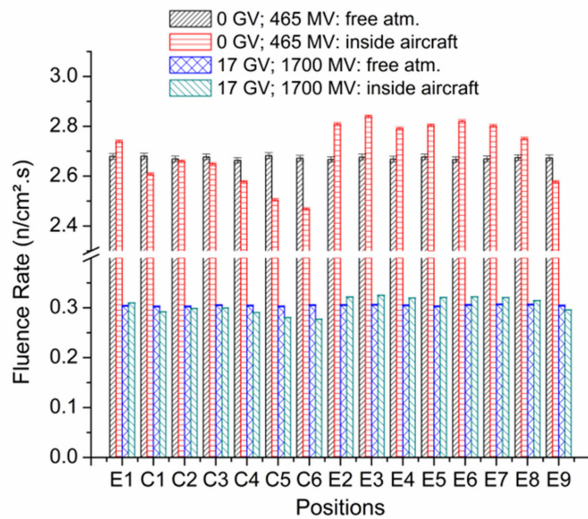


Fig. 8. Fluence rate of neutrons with energies above 1 MeV at 11-km of altitude.

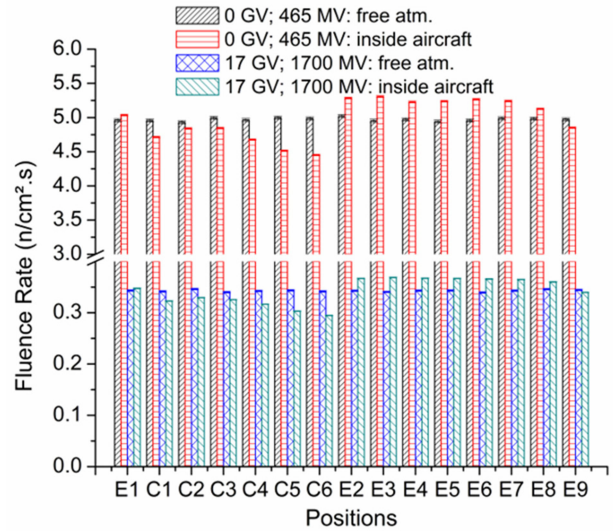


Fig. 9. Fluence rate of neutrons with energies above 1 MeV at 18-km of altitude.

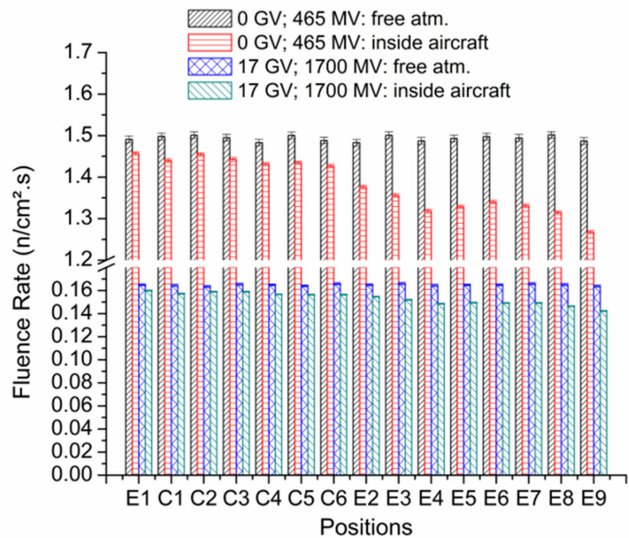


Fig. 10. Fluence rate of neutrons with energies above 10 MeV at 11-km of altitude.

E1–E8 for both equatorial and polar region altitudes. The highest fluence rates occur in positions at the bottom of the aircraft, except for the position E9.

For polar routes, flights at 18-km altitude present a fluence rate of neutrons with energy above 1 MeV 1.85 times higher than flights at 11-km altitude, whereas for equatorial flights at 18-km altitude this difference is reduced to a 1.13 factor. This implies that the neutron fluence rate with energy higher than 1 MeV increase more with the altitude at polar routes than at the equatorial routes.

Figs. 10 and 11 show the fluence rate for neutrons with energy above 10 MeV, for 11- and 18-km, respectively.

For both, 11- and 18-km altitude, the neutrons fluence rate with energy above 10 MeV is smaller inside the aircraft than at free atmosphere. This occurs due to the aircraft's

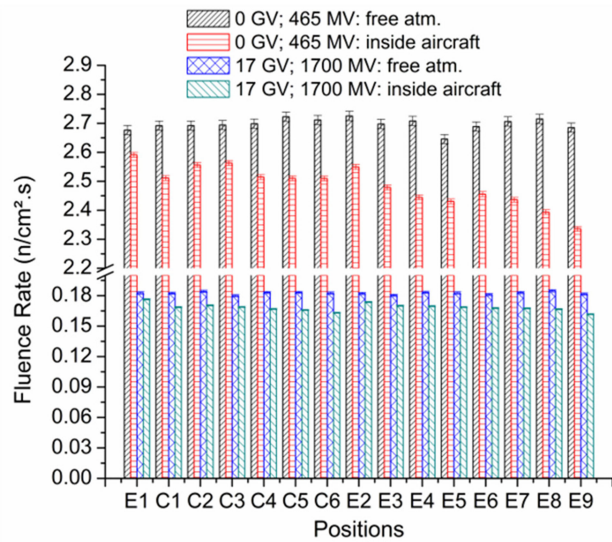


Fig. 11. Fluence rate of neutrons with energies above 10 MeV at 18-km of altitude.

TABLE III
Maximum Variation of Neutron Fluence Rate Between Different Positions Inside the Aircraft

Altitude	E > 1 MeV		E > 10 MeV	
	Pole	Equator	Pole	Equator
11 km	15%	20%	14%	13%
18 km	16%	21%	10%	9%

shielding effect and it is associated with the energy reduction of its particles for this radiation field.

For energies greater than 1 MeV, the results showed an increase or decrease in the neutron fluence, depending on the position inside the aircraft. Table III summarizes the maximum variation between different positions inside the aircraft, for both situations (pole and equator) and for both energy thresholds ($E > 1$ MeV and $E > 10$ MeV).

Table III shows a tendency of higher differences on the neutron fluence rate between the positions inside the aircraft for lower energy threshold ($E > 1$ MeV) in comparison with those differences for higher energy threshold ($E > 10$ MeV). One can also observe that the difference is even higher in the equator region, compared to the polar region.

Thus, it indicates that devices with new technologies below 150 nm are more susceptible to radiation effects such as SEE than devices with older technologies due to the latitude effects resulting from their lower SEE threshold (around 1 MeV, or less). This analysis allows inferring that the adoption of new technologies may amplify discrepancies between the SEE rate in equatorial regions and in polar regions and also in the positioning of the device in the aircraft, with consequent impact for aircraft safety.

2) *Energy Spectrum Evaluation:* An evaluation of the energy spectrum was made in different positions inside the aircraft for each of the two routes previously presented. This section shows the analysis of three positions: avionics, near the fuel and at the bottom of the aircraft positions. Figs. 12

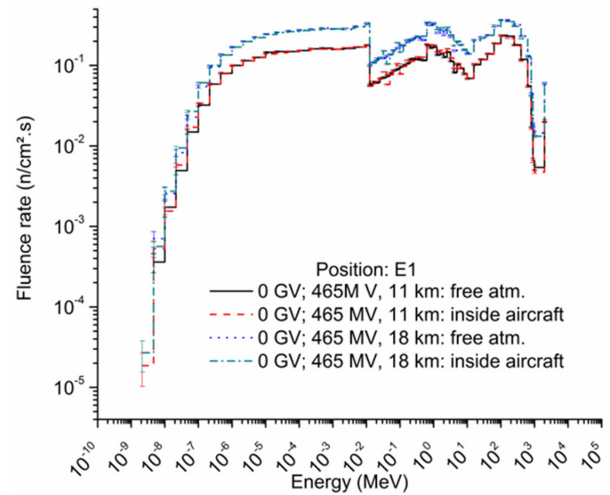


Fig. 12. Fluence rate of neutron as function of energy for polar route flights at E1 position.

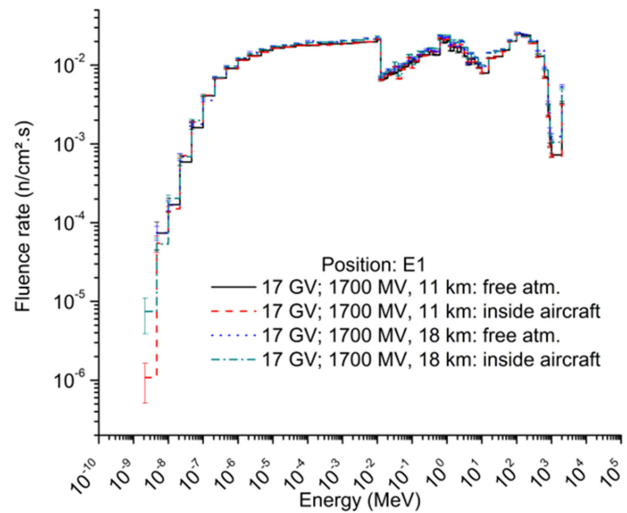


Fig. 13. Fluence rate of neutron as function of energy for equatorial route flights in E1 position.

and 13 show the fluence rate of neutrons in the position E1 as a function of the energy for the polar route during a solar minimum and for the equatorial route during a solar maximum, respectively. The discontinuity presented results from the change of the energy bins size.

One can observe no significant differences between the neutron spectrum inside the aircraft and in the free atmosphere, probably due to the position close to the nose of aircraft.

Figs. 14 and 15 show the fluence rate as a function of the energy for the polar route during a solar minimum and equatorial route during a solar maximum, respectively, in position C6. In position, which is close to the fuel, there is a sizable production of thermal neutrons. One can observe that the thermal neutron fluence rate inside the aircraft is approximately two orders of magnitude greater than the fluence rate at free atmosphere for all conditions of flight and altitudes evaluated.

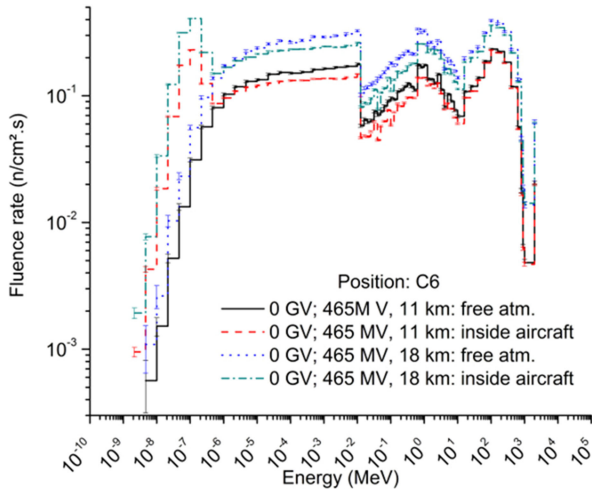


Fig. 14. Fluence rate of neutron as function of energy for polar route flights at C6 position.

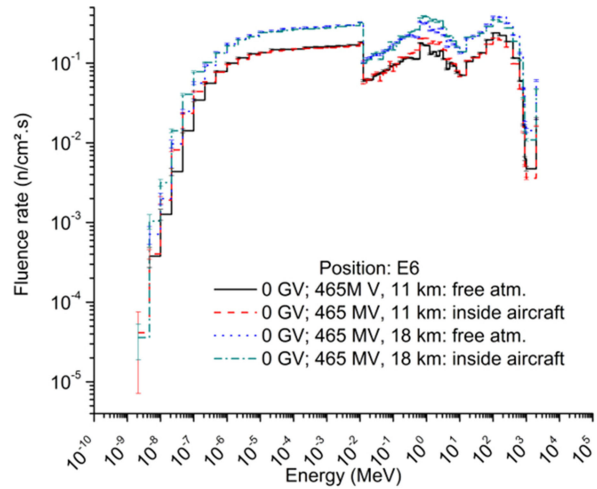


Fig. 16. Fluence rate of neutron as function of energy for polar route flights at E6 position.

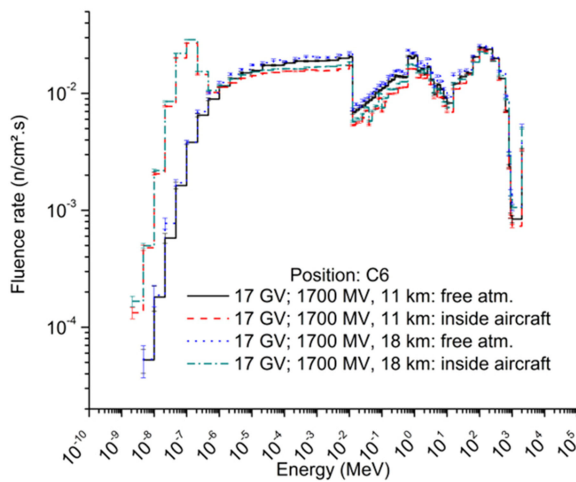


Fig. 15. Fluence rate of neutron as function of energy for equatorial route flights in C6 position.

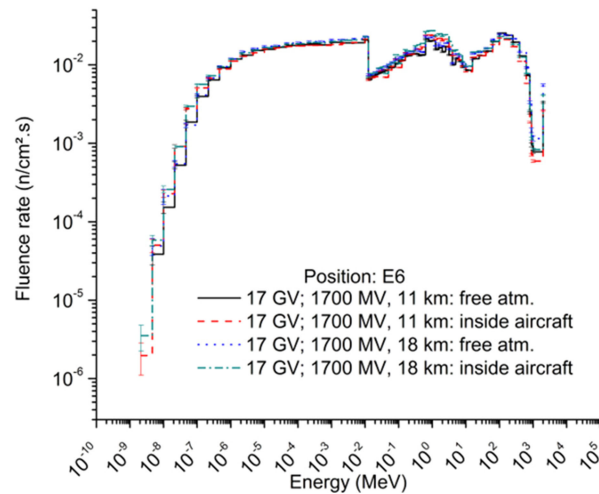


Fig. 17. Fluence rate of neutron as function of energy for equatorial route flights in E6 position.

Neutrons with energies above 1 MeV in C6 position do not show significant differences in fluence rate, being the number of neutrons inside the aircraft, in general, slightly lower than at the free atmosphere for both conditions and altitudes of the flight studied.

Figs. 16 and 17 show the fluence rate as a function of energy for polar route during minimum solar and equatorial route during maximum solar, respectively, at the E6 position.

The detector in the position E6 is located at the bottom of the aircraft near many different materials which can scatter the radiation around it. Due to the thermal neutron production inside the aircraft for all routes and altitudes of flight, the thermal neutron fluence rate inside the aircraft is four times higher than the fluence rate at the free atmosphere.

The behavior shown in Figs. 14 and 15 represent the other positions near hydrogenated materials, such as the human body; therefore, the results at this position (C6) are also representative of positions C1–C6.

In the same way, the behavior shown in Figs. 16 and 17 represent other positions located at the bottom of the aircraft, near structural and cargo materials (positions E2–E9).

Table IV shows the ratio between the thermal and neutrons with energy greater than 10 MeV neutron fluence results in comparison to our simulations and some experimental data from the literature for some different conditions [2].

3) *Analysis of the Angular Distribution of Neutrons Within the Aircraft:* The analysis of the angular distribution is important to identify how the aircraft's materials affect the direction of incident neutrons that hit the avionics devices.

This information is relevant not only to consider the position to install the avionics within the aircraft, to reduce its failure probability but also to assess the most favorable orientation for the devices, considering the probability of multiple cell upsets (MCUs) occurrence and multiple bit upsets (MBUs) in the component. The MCUs and MBUs

TABLE IV
Comparisons of the Ratio of Thermal and High Energy Neutron
($E > 10$ MeV) Fluence Rate

Researcher	Position	Altitude (km)	Ratio Thermal / $E > 10$ MeV
Hubert ¹		10.6	0.5
Goldhagen ¹		12.2	0.24
Nakamura ¹		11.3	0.49
Armstrong ¹	Free atm.	11.9	0.2
Simulation ²	Free atm.	11.0	0.19
Inside aircraft in equatorial region ²	E1	11.0	0.21
	C6	11.0	0.60
Inside aircraft in polar region ²	E1	11.0	0.20
	C6	11.0	0.56

¹Experimental data from [2].²Results from simulations developed in this work.

are kinds of SEE and they are similar to the SEU but the upset occurs in many bits in the same word (MBU) or in different words that are close to each other (MCU).

The analysis was made using the reference system in which the angle of 0° corresponds to the particles moving in the upward direction, so, for all analysis, the neutrons with an angular range of 180° to 120° is considered downward direction, from 120° to 60° is considered lateral direction and from 60° to 0° is considered upward direction.

Figs. 18 and 19 show the fluence rate of neutrons as a function of its incidence angle for the polar route during the solar minimum and for the equatorial route during solar maximum, respectively, in the position E1.

The E1 position shows an increase in the number of neutrons with angles from 80° to 120° inside the aircraft for flights at 18-km altitude on the equatorial route and this increase for polar routes happens for angles from 90° . At 11-km altitude, the increase inside the aircraft occurs for neutrons with angles from 100° for both routes estimates.

As presented in Fig. 19, one can observe that equatorial flights at 11-km altitude have a slightly larger quantity of neutrons inside the aircraft, becoming greater than the ones at 18-km altitude, for particles that reach the device in the downward direction, at angles between 135° and 180° .

Figs. 20 and 21 present the neutrons fluence rate as a function of its incidence angle for the polar route during solar minimum and equatorial route during solar maximum, respectively, in the C6 position.

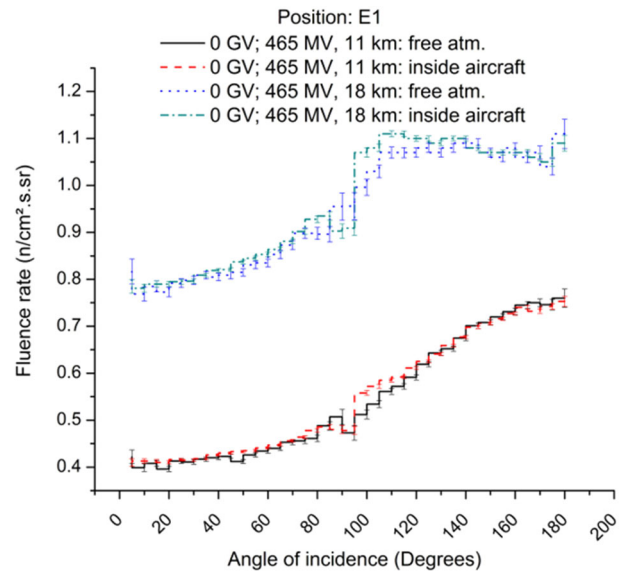


Fig. 18. Fluence rate of neutron as function of its incidence angle for polar route flights in E1 position.

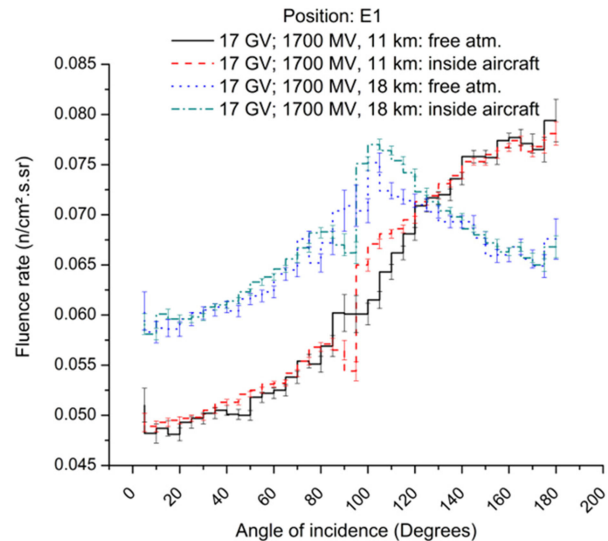


Fig. 19. Fluence rate of neutron as function of its incidence angle for equatorial route flights at E1 position.

In the position C6, which is near hydrogenated materials, on the polar route at both altitudes, the quantity of neutrons with directions from 20° to 40° and above 120° is similar inside and outside the aircraft; however, this difference is very small.

As it is shown in Fig. 21, at this position the equatorial route at 18-km altitude has a higher concentration of neutrons with directions from 90° to 130° , whereas flights at 11-km altitude, the neutron fluence rate becomes greater than the one at 18-km altitude for angles larger than 135° . Also, in this position, the total amount of neutrons at the free atmosphere is higher than inside the aircraft.

Figs. 22 and 23 show the fluence rate of the neutron as a function of its incidence angle for the polar route during

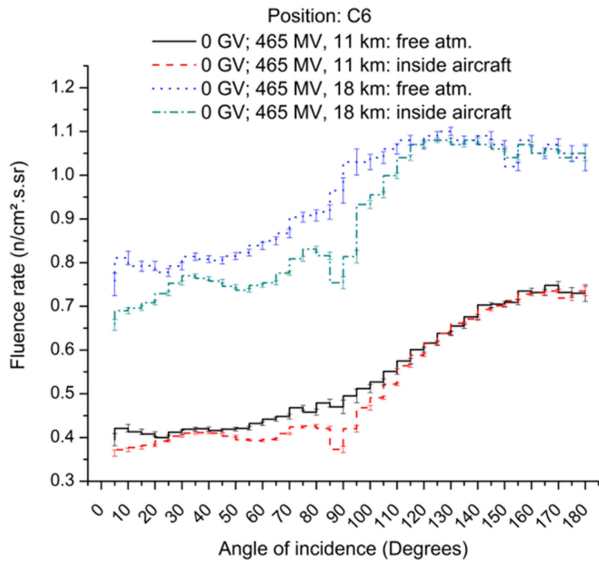


Fig. 20. Fluence rate of neutron as function of its incidence angle for polar route flights in C6 position.

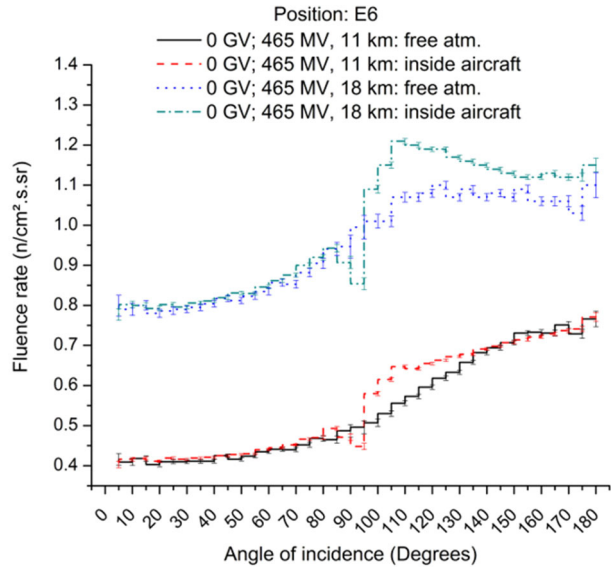


Fig. 22. Fluence rate of neutron as function of its incidence angle for polar route flights at E6 position.

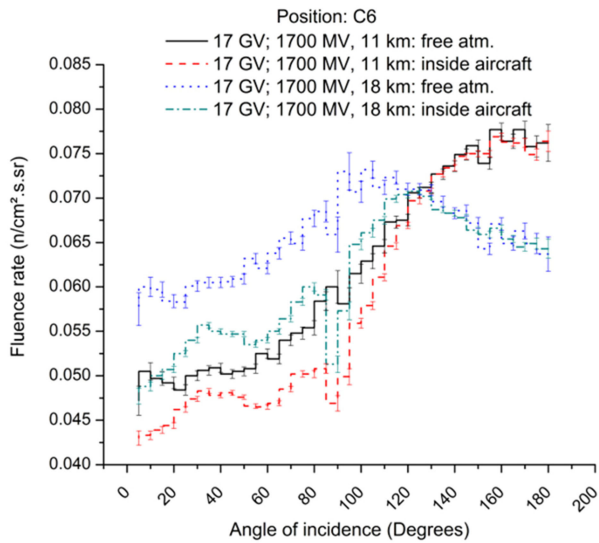


Fig. 21. Fluence rate of neutron as function of its incidence angle for equatorial route flights at C6 position.

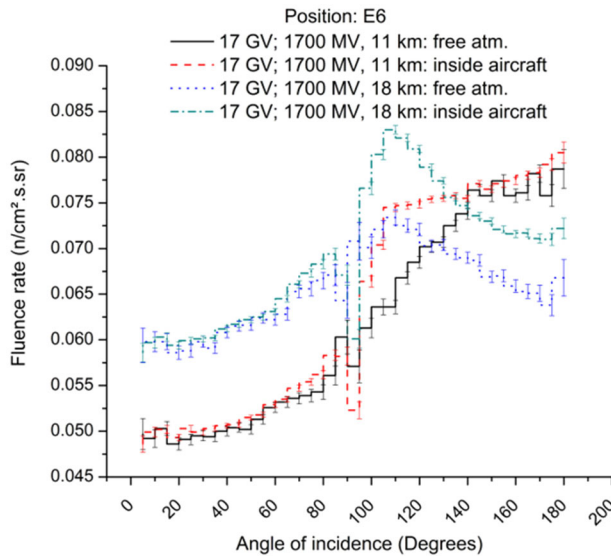


Fig. 23. Fluence rate of neutron as function of its incidence angle for equatorial route flights at E6 position.

a solar minimum and for the equatorial route during a solar maximum, respectively, in the position E6.

At this position, the neutron fluence inside the aircraft is greater than at free atmosphere for particle incident with angles above 100° for both routes at 18-km altitude.

For flights on polar routes and 11-km altitude, the difference between the neutron fluence rates inside and outside the aircraft are small, except in the angular range from 95° to 130° . For this range, the amount of neutrons inside the aircraft is noticeably higher than in the free atmosphere.

On flights at the same altitude but on equatorial routes, the amount of neutrons is larger inside the aircraft for angles from 100° to 145° .

From Figs. 22 and 23, it is possible to conclude that for all flight conditions the direction of neutron incidence is

predominantly downward compared to upward and lateral directions.

From the results presented in this section, we observed how the angular distribution of particles inside the aircraft depends on the position and the material around it. It is known that the neutron fluence rate is different in each angular range and this information should be considered when designing the position and orientation of an avionics device in the aircraft, since depending on them, it will be subject to a given fluence of neutrons, which in turn will determine the rate of MBUS and MCUs, thus affecting its expected failure rate.

TABLE V
Neutron Counting Ratio (Vertical/Horizontal Detector) for Three Ranges of Neutron Energy (11-km)

Position	E1	C6
E < 1 eV	1.07	1.18
E > 1 MeV	0.99	0.89
E > 10 MeV	0.92	0.86

TABLE VI
Neutron Counting Ratio (Vertical/Horizontal Detector) for Three Ranges of Neutron Energy (18-km)

Position	E1	C6
E < 1 eV	1.08	1.18
E > 1 MeV	1.12	1.02
E > 10 MeV	1.17	1.10

C. Orientation of the Device Inside the Aircraft

The results previously shown refer to a detector surface in a horizontal position. Other simulations were performed using a detector surface in a vertical position to investigate if the avionics device orientation can affect the neutron amount that hits the device due to anisotropies on the angular distribution of neutron fluence inside the aircraft.

The results presented in this section is for the equatorial region (17 GV), in a solar maximum period (1700 MV) at 11- and 18-km altitude. Only fluences in two positions were evaluated for analyzes in this section, one concerning the avionics compartment (E1) and the other near the fuel (C6).

Tables V and VI show the ratio of neutron counts on the detector surface inside the aircraft from the vertical detector in relation to the horizontal detector at 11- and 18-km altitude, respectively, for three energy regions for positions E1 and C6.

In Table V, for thermal energy neutrons, the vertical detector counts 18% more neutrons than the horizontal for both positions evaluated. For neutron with energies above 1 MeV and neutrons with high energy above 10 MeV, the horizontal detector counts more neutrons than the vertical, for both positions, and consequently, for these energy ranges, this position is related to a bigger amount of neutrons impinging the detector.

The difference between neutron counts on the horizontal and vertical detector for positions near the fuel or hydrogenated materials, such as position C6, can be up to 1.2 times higher on a vertical detector than in a horizontal detector inside the aircraft. The opposite behavior is observed for higher energy neutrons.

In Table VI, we show the analyses at 18-km altitude. The vertical detector counts more neutrons than the horizontal detector for all energy ranges evaluated. The neutron counting ratio (vertical/horizontal detector) is a function of neutron energy, but as well a function of altitude as we can observe in Tables V and VI.

As observed in Tables V and VI, the neutron radiation field anisotropy inside the aircraft may imply significant differences in the neutron incident amount on devices positioned in different orientations. These differences in the neutron amount and incidence angle may result in variations of the SEE rate, as well as may affect MBU and MCU rates differently, due to the impact of device orientation on the MCU radiation response in nanoscale integrated circuits [23].

IV. CONCLUSION

The aircraft model built on MCNPX allows evaluating the behavior of the radiation field inside the aircraft considering a realistic neutron fluence rate found at the atmosphere using data from gParAt platform. We performed simulations considering the equatorial and polar regions and the altitudes of 11- and 18-km.

From our simulations, we reach the following conclusions about the neutron fluence rate inside aircraft.

- 1) At 11- and 18-km altitude, there is a maximum increasing about 190% in the thermal neutron fluence rate at different positions inside the aircraft compared to the thermal neutron fluence rate in the free atmosphere.
- 2) For neutrons with energies greater than 1 MeV and both altitudes, the neutron fluence rate depends on their position and it is higher inside the aircraft than at a free atmosphere for many positions evaluated. These differences vary from a decrease of 12% to an increase of 9%.
- 3) For neutrons with energies above 10 MeV, the fluence rate inside aircraft decrease for all positions compared to the free atmosphere, and the maximum variation is 15% found in the E9 position (close to the fuel). This behavior was observed for both equatorial and polar regions.
- 4) The maximum variation of neutron fluence rate between different positions inside the aircraft shows a tendency of higher differences for lower energy threshold ($E > 1$ MeV) in comparison with those differences for higher energy threshold ($E > 10$ MeV). This difference is even higher in the equator region compared to the polar region.

Summarizing the above conclusions, one can see a tendency for new technologies to be more susceptible to positioning inside the aircraft due to higher variations for neutron fluence rate above 1 MeV. For newer technologies, which are susceptible to energies above 0.5 MeV, this situation could be even more relevant. Moreover, this analysis allows inferring that the adoption of new technologies may amplify discrepancies between the SEE rate in equatorial regions and polar regions with consequent impact for aircraft safety.

We reach the following conclusions about the neutron angular neutron distribution inside aircraft.

- 1) The incidence angle of neutrons depends on the position inside the aircraft, and the proximity of highly hydrogenated materials, such as fuel and passengers, is the main factor that changes the angular distribution (see Fig. 21). This is rarely addressed in the literature, although its importance is clear, especially in the rate of MCU and MBU that could depend on the particle incidence direction.
- 2) The differences in the fluence angular distribution per solid angle between the free atmosphere and inside the aircraft range from 78% up to 117% depending on neutron energy and position inside the aircraft (see Fig. 21).
- 3) The neutron radiation field anisotropy inside the aircraft may imply differences in the neutron incident amount on devices positioned in different orientations varies from a decrease of 14% to an increase of 18% at 11-km altitude (see Table IV) and from increases of 2% to 18% at 18-km altitude (see Table V).

From these analyses, we demonstrated that there are differences in the angular distribution inside the aircraft, depending on position and neutron energy distribution. Such differences, which could induce variations in the failure probability of avionics devices, are not considered in the usual safety evaluation methodology for aircrafts.

The neutron fluence rate and angular distribution are partially affected by positions inside the aircraft and flight regions. The sum of these contributions could result in a significant minimization of the expected failure probability of avionics devices, but this approach is rarely addressed in the literature.

This type of computational previous evaluation can be favorably used for safety if this type of assessment is introduced in the step of positioning the devices during the aircraft design, introducing a low-cost stage with potentially significant results for the reduction of radiation-induced failure in onboard electronic systems, especially for newer technologies.

REFERENCES

- [1] M. M. Meier and D. Matthiä
A space weather index for the radiation field at aviation altitudes
J. Space Weather Space Climate, vol. 4, no. A13, pp. 1–5, 2014, doi: [10.1051/swsc/2014010](https://doi.org/10.1051/swsc/2014010).
- [2] *Process Management for Avionics—Atmospheric Radiation Effects—Part 1: Accommodation of Atmospheric Radiation Effects via Single Event Effects Within Avionics Electronic Equipment*, IEC 62396-1, International Electrotechnical Commission, Geneva, Switzerland, 2016.
- [3] C. Dyer and F. Lei
Monte Carlo calculations of the influence on aircraft radiation environments of structures and solar particle events
IEEE Trans. Nucl. Sci., vol. 48, no. 6, pp. 1987–1995, Dec. 2001.
- [4] R. A. Weller *et al.*
Monte Carlo simulation of single event effects
IEEE Trans. Nucl. Sci., vol. 57, no. 4, pp. 1726–1746, Aug. 2010.
- [5] J. L. Aufran, S. Semikh, D. Munteanu, G. Gasiot, and P. Roche
Soft-error rate induced by thermal and low energy neutrons in 40 nm SRAMs
IEEE Trans. Nucl. Sci., vol. 59, no. 6, pp. 2658–2665, Dec. 2012.
- [6] A. Ferrari, M. Pelliccioni, and R. Villari
Evaluation of the influence of aircraft shielding on the aircrew exposure through an aircraft mathematical model
Radiat. Protection Dosimetry, vol. 108, no. 2, pp. 91–105, 2004.
- [7] A. Ferrari, M. Pelliccioni, and R. Villari
A mathematical model of aircraft for evaluating the effects of shielding structure on aircrew exposure
Radiat. Protection Dosimetry, vol. 116, no. 1/4, pp. 331–335, 2005.
- [8] G. Battistoni, A. Ferrari, M. Pelliccioni, and R. Villari
Monte Carlo calculation of the angular distribution of cosmic rays at flight altitudes
Radiat. Protection Dosimetry, vol. 112, no. 3, pp. 331–343, 2004.
- [9] G. Battistoni, A. Ferrari, M. Pelliccioni, and R. Villari
Evaluation of the doses to aircrew members taking into consideration the aircraft structures
Adv. Space Res., vol. 36, pp. 1645–1652, 2005.
- [10] J. Kubančák, I. Ambrožová, O. Ploc, K. P. Brabcová, V. Štěpán, and Y. Uchihori
Measurement of dose equivalent distribution on-board commercial jet aircraft
Radiat. Protection Dosimetry, vol. 162, no. 3, pp. 215–219, 2014.
- [11] G. Hubert, P. Trochet, O. Riant, P. Heinz, and R. Gaillard
A neutron spectrometer for avionic environment investigations
IEEE Trans. Nucl. Sci., vol. 51, no. 6, pp. 3452–3456, Dec. 2004.
- [12] T. Nakamura *et al.*
Altitude variation of cosmic ray neutrons
Health Phys., vol. 53, pp. 509–517, 1987.
- [13] J. Hewitt *et al.*
Ames collaborative study of cosmic ray neutrons: Mid-latitude flights
Health Phys., vol. 34, pp. 375–384, 1978.
- [14] D. Pelowitz
“MCNPX user’s manual version 2.5.0,” Los Alamos National Laboratory, Los Alamos, NM, USA, Rep. LA-CP-05-0369, 2005.
- [15] J. C. Dalazen
FAB 2717 / VU35A Learjet / 1° Grupo De Transporte Especial, 2009. Accessed: Feb. 6, 2014. [Online]. Available: <http://www.flickr.com/photos/aviao/3405103247/>
- [16] A. C. M. Prado *et al.*
Investigation of the influence of the position inside a small aircraft on the cosmic-ray-induced dose
Radiat. Protection Dosimetry, vol. 176, no. 3, pp. 217–225, 2017.
- [17] National Institute of Standards and Technology, “Atomic weights and isotopic compositions for all elements,” Accessed: Apr. 23, 2015. [Online]. Available: http://physics.nist.gov/cgi-bin/Compositions/stand_alone.pl?ele=&all=all&ascii=html&isotype=some/
- [18] ENDF-6 *Formats Manual* IAEA-NDS-76, 5 ed., Int. Atomic Energy Agency, Vienna, Austria, 2001.

- [19] M.T. Pazianotto *et al.*
Extensive air shower Monte Carlo modeling at the ground and aircraft flight altitude in the South Atlantic magnetic anomaly and comparison with neutron measurements
Astropart. Phys., vol. 88, pp. 17–29, 2017.
- [20] M.T. Pazianotto *et al.*
Analysis of the angular distribution of cosmic-ray-induced particles in the atmosphere based on Monte Carlo simulations including the influence of the Earth’s magnetic field
Astropart. Phys., vol. 97, pp. 106–117, 2018.
- [21] L. Koops
Cosmic radiation exposure of future hypersonic flight missions
Radiat. Protection Dosimetry, vol. 175, no. 2, pp. 267–278, 2017.
- [22] F. H. Attix
Introduction to Radiological Physics and Radiation Dosimetry. Wiley-VCH, Weinheim, Germany, 1986.
- [23] A. D. Tipton
On the impact of device orientation on the Multiple Cell Upset radiation response in nanoscale integrated circuits
Ph.D. dissertation, Dept. Elect. Eng., Vanderbilt Univ., Nashville, TN, USA, 2008.



Adriane Cristina Mendes Prado was born in São Jose dos Campos, Brazil, in 1990. She received the bachelor’s degree in aerospace engineering from the Vale do Paraíba University, São José dos Campos, Brazil, in 2012, and the M.S. degree in space science and technologies in 2015 from the Technological Institute of Aeronautics (ITA), São Jose dos Campos, Brazil, where she is currently working toward the Ph.D. degree in space science and technologies in the area of physics and mathematics advances.

Since 2010, she has been a Collaborator with the Institute for Advanced Studies (IEAv) of the Aerospace Science and Technology Department (DCTA), the Brazilian Air Force. She has worked in flight tests with radiation detection equipment, checking cosmic radiation in crew and aircraft, having knowledge of how radiation interferes in electronic systems and Monte Carlo simulations of cosmic radiation. Her research interests include the cosmic radiation dosimetry, neutron and cosmic particle scattering inside the aircraft with Monte Carlo simulation, and radiation effects on avionics systems.



Maurício Tizziani Pazianotto received the B.S. degree in medical physics from the São Paulo State University (UNESP), São Paulo, Brazil, in 2009, and the Ph.D. degree in nuclear physics from the Technological Institute of Aeronautics (ITA), So Jos dos Campos, Brazil, in December 2015.

From 2012 to 2013, he had a doctoral stay at the University of Seville, Spain. During his Ph.D. work, he modeled and measured the spectra and the ambient dose equivalent rate of neutrons at flight altitude in the South America Magnetic Anomaly. He has developed simulations of the cosmic radiation transport and particle detectors for aeronautical interest.



José Manuel Quesada Molina received the degree in physics in 1982 and the Ph.D. degree in physics in 1985, both from the University of Seville, Seville, Spain.

During 1983–1985, he did his Ph.D. research on theory of heavy ion collisions at the Niels Bohr Institute of the University of Copenhagen, Denmark. In 1987, he joined the Department of Atomic, Molecular and Nuclear Physics, University of Seville, where he is currently a Full Professor. During 1989–1990, he was a Scientific Associate with the Hadron Injector Group, Proton Synchrotron Division, CERN, where he contributed to the design of beam dynamics-related aspects of the lead ion RFQ. He is team leader of the University of Seville's Group participating in the n_TOF experiment at CERN for the measurement of neutron cross sections of interest in technology and nuclear astrophysics, since its inception in 2000. He pioneered the participation of the University of Seville's Group in the Geant4 Collaboration since 2007, where he contributes to the development and maintenance of the low-energy hadronic models. He has worked on the development of Geant4 applications in the domains of neutron spallation reactions, radiotherapy, microelectronics, and aerospace technology. In connection to the last aspect, he has been a Visiting Senior Scientist with the Technological Institute of Aeronautics, Brazil. Simultaneously, he has continued his work on nuclear reaction theory through the development of a nuclear potential for nucleon–nucleus scattering well suited for applications. He has participated as national representative in several coordinated research projects and technical meetings organized by the IAEA related to medical applications of nuclear data. He has authored or coauthored more than 280 publications in peer-reviewed journals and conference proceedings.

Dr. Quesada has been a Principal Investigator of research projects with national and international (EU) funding.



Miguel Antonio Cortés-Giraldo received the B.S. and Ph.D. degrees in physics from the University of Seville, Seville, Spain, in 2006 and 2011, respectively.

Since 2019, he has been an Associate Professor with the Department of Atomic, Molecular and Nuclear Physics, University of Seville, where he was an Assistant Professor from 2011 to 2019. He has authored more than 40 scientific articles, one invention, and one book on biophysics for the general public. His research interests include track structure Monte Carlo simulations, Monte Carlo calculations applied to microdosimetry and radiobiology in proton therapy, Monte Carlo modeling of neutron transport and of radiation detectors.

Dr. Cortés-Giraldo is a member of the Geant4 since 2007, n_TOF since 2009, and Geant4-DNA since 2019. He was the recipient of the Best Poster Award on Novel Technologies in Radiation Therapy at the ICTR-PHE 2012 Conference and was recognized as Outstanding Reviewer of *European Journal of Medical Physics – Physica Medica*. He has also received several awards and honors from regional institutions.



Guillaume Hubert received the M.S. degree in materials sciences and solid state physics from the Pierre et Marie Curie University (Paris VI), Paris, France, the Ph.D. degree from the Montpellier University, Montpellier, France, in 2002, and the capacitance to supervise Ph.D. from the Toulouse University, Toulouse, France, in 2010.

During his doctoral studies, he developed a predictive methodology dedicated to the single-event upset induced by the neutron atmospheric. From 2002 to 2007, he was a Research Physicist with European Aeronautic Defense and System (EADS) Group. In 2007, he joined ONERA (the French Aerospace Laboratory), Physics, Instrumentation, Environment and Space Department (DPHY) rays. His research interests include single-event effect modeling based on multiphysics, and atmospheric radiation environment studies based on world-network operating cosmic ray spectrometers in high-altitude, and nuclear transport simulations applied to atmospheric air-showers modeling. He is the author and co-author of more than 120 international journal publications and conference proceeding in the fields of SEE and cosmic. He participates or has participated in several international or national research projects.

Dr. Hubert is currently a Principal Investigator of the CHINSTRAP Polar Project in which he has conducted three summer campaigns in Antarctica.



Marlon Antonio Pereira was born in Jacareí, Brazil in 1975. He received the bachelor's degree in chemical engineering, and the M.S. and Ph.D. degrees in space sciences and technologies from the Technological Institute of Aeronautics (ITA), São Jose dos Campos, Brazil, in 1992, 2013, and 2017, respectively.

Since 2014, he has been a Radioprotection Assistant with the Institute for Advanced Studies (IEAv), Aerospace Science and Technology Department (DCTA), Brazilian Air Force. He is also a Research Assistant with the Aerospace Dosimetry Laboratory (LDA), IEAv, DCTA, in the radiation measurements, cosmic radiation dosimetry, and its effects.



Claudio Antonio Federico was born in São Paulo, Brazil, in 1969. He received the bachelor's degree in physics, and the master's and Ph.D. degrees in nuclear technology from São Paulo University, São Paulo, Brazil, in 1992, 2003, and 2011, respectively.

Since 1994, he has been with the Institute for Advanced Studies (IEAv), Aerospace Science and Technology Department (DCTA), Brazilian Air Force, as a Radiation Safety Officer and Researcher. He has experience in physics, with emphasis on radiation measurement, cosmic radiation dosimetry, neutron dosimetry, radiation protection, and cosmic radiation effects. He is currently the Head of Aerospace Dosimetry Laboratory (LDA), IEAv/DCTA, and also, a Permanent Professor and Advisor on the Space Sciences and Technologies Postgraduate Program (master's and doctorate) with the Technological Institute of Aeronautics (ITA), São Jose dos Campos, Brazil.